LWT - Food Science and Technology 155 (2022) 113001

Contents lists available at ScienceDirect

LWT

journal homepage: www.elsevier.com/locate/lwt

Nuclear Magnetic Resonance (NMR) study of Palm Kernel Stearin: Effects of cooling rate on crystallization behaviour

Ilhami Okur [a,b], Baris Ozel [a,c], Derya Ucbas [a,d], Leonid Grunin [e,f], Purlen Sezer Okur [a], Hami Alpas [a], Semra Ide [g], Mecit Halil Oztop [a,*]

[a] Department of Food Engineering, Middle East Technical University, 06800, Ankara, Turkey
[b] Department of Food Engineering, Nigde Omer Halisdemir University, 51240, Nigde, Turkey
[c] Department of Food Engineering, Ahi Evran University, 40100, Kirsehir, Turkey
[d] Department of Food Engineering, Eskisehir Osmangazi University, 26040, Eskisehir, Turkey
[e] Resonance Systems GmbH, Kircheim/Treck, Germany
[f] Department of Physics, Volga State University of Technology, 424000, Yoshkar-Ola, Russia
[g] Hacettepe University, Physics Engineering, Ankara, Turkey

ARTICLE INFO

Keywords:
^{1}H NMR
Palm kernel stearin
Crystal polymorph
X-ray scattering
Wide angle X-ray scattering (WAXS)

ABSTRACT

In this study, effects of different cooling rates (0.5,3.3,4.7 and 6.9 °C/min) on the crystallization behavior of palm-kernel-stearin (PKS) were studied by low-field NMR relaxometry. According to results, solid fat content (SFC), longitudinal relaxation time (T_1), second moment (M_2) and degree of crystallinity (%) of the samples increased with increase in cooling rate from 0.5 to 6.9 °C/min. In contrast, transverse relaxation time (T_2) demonstrated an opposite behavior with respect to T_1 and decreased when the cooling rate increased. Additionally, effects of cooling rate on the changes of polymorph structures were detected by X-ray measurements. Degree of crystallinity showed high Pearson correlation values ($\alpha \leq 0.05$) with SFC ($r = 0.771$) and T_1($r = 0.932$). Changes in the crystal polymorphs could also be explained by NMR parameters to some extent as can be observed by the strong correlation between the β crystal content and T_2 ($r = 0.927$). At the highest cooling rate, β′ crystals were the dominant polymorphic form and constituted 75(%) of the total crystals present. Results of this study suggested that NMR relaxometry could be used as a complementary tool to interpret the crystallization behavior of PKS.

1. Introduction

Palm Kernel Stearin (PKS), a stearin fraction of palm kernel oil with high lauric acid (56%) and myristic acid (21%) content, is composed of various saturated triglycerides (TAGs). Caprylic, capric, palmitic and stearic acids constitute the rest of the total fatty acids (FAs) present in PKS (Goon, Abdul Kadir, Latip, Rahim, & Mazlan, 2019). Due to its high saturated FAs content and the resulting sharp melting behavior, PKS is widely utilized in confectionary products (X. Zhang et al., 2013). Moreover, when used in formulations, PKS imparts satisfactory mouth-feel characteristics so that it could be used in food products including cooking/frying oil, margarine, shortenings, fat spreads, ice-creams, cheese analogues, animal fat replacers, mayonnaise, salad dressings and coconut milk analogues (Dian et al., 2017; Norizzah, Nur Azimah, & Zaliha, 2018). PKS is also commonly used in the chocolate industry as a cocoa butter replacer due to its high lauric acid content (F. Wang et al., 2011).

Crystallization studies of fat systems have a great scientific and practical importance as stated in previous reports since the determination of fat crystallization behaviors enables the control of industrial operations that lead to desirable texture in the final lipid containing products. Each lipid has distinct crystallization behavior promoting different three-dimensional arrangements in their fat crystalline network in terms of the degree of order and state of polymorphism of fat crystals. Fat crystalline characteristics have major effects on the physical and functional properties of food products. Therefore, analysis of fat crystallization is at utmost importance in such products (Chaleepa, Szepes, & Ulrich, 2010; Himawan, Starov, & Stapley, 2006; Maleky, Acevedo, & Marangoni, 2012). Crystal structure and crystallization phenomena are greatly affected by many factors such as cooling rate,

* Corresponding author. Middle East Technical University, Engineering Faculty, Food Engineering Department, Ankara, Turkey.
E-mail address: mecit@metu.edu.tr (M.H. Oztop).

https://doi.org/10.1016/j.lwt.2021.113001
Received 6 July 2021; Received in revised form 13 December 2021; Accepted 16 December 2021
Available online 19 December 2021

fatty acid chain length and composition, TAG organization and some processing conditions *e.g.* rate of agitation. Changes in the cooling rate might also affect the microstructural characteristic via controlling the nucleation and growth rates of the crystals (Gregersen, Miller, Hammershøj, Andersen, & Wiking, 2015; Sato, Bayés-García, Calvet, Cuevas-Diarte, & Ueno, 2013).

Nuclear Magnetic Resonance (NMR) relaxometry is a rapid and non-destructive method to interpret physicochemical changes in food systems (H. Zhang, Zhang, Sun, & Xie, 2015). With ^{1}H NMR relaxometry, it is possible to get information about different proton compartments of the food systems that show detailed information about the complex structure of such systems (Kirtil & Oztop, 2016). Time domain (TD) NMR is generally based on measurements of relaxation times through different pulse sequences, known as longitudinal relaxation time (spin-lattice relaxation time, T_1) and transverse relaxation time (spin-spin relaxation time, T_2) and these relaxation times are related to physicochemical changes in food systems (Alacik Develioglu, Ozel, Sahin, & Oztop, 2020). Although slow dynamics of the solid fat phase restricts the use of TD NMR for detection of fat polymorphism purposes, relaxation time measurements still have some potential for the investigation of fat polymorphism and crystal size distribution when combined with different preexisting experimental methods (H. Zhang et al., 2015). Spin-lattice relaxation time is more sensitive to the changes in the organizations of the crystalline state such as the variations in the crystal packing arrangements whereas spin-spin relaxation time is suitable to monitor the semi-solid behaviors of lipids in the whole sample volume (M. Adam-Berret, Rondeau-Mouro, Riaublanc, & Mariette, 2008). The dipolar second moment (M_2) is another important measurement of TD NMR which can characterize the proton mobility in polycrystalline solid samples (Grunin, Oztop, Guner, & Baltaci, 2019). M_2 is related to the magnetic dipole-dipole interactions in immobile systems. Measurement of M_2 in solid state of lipid systems could be considered as an alternative to T_2. For solids, the transverse relaxation decay behaves normally out of any classical models, so the integration of the second moment in frequency domain area becomes more precise than fitting of time-domain signals with a definite function. In previous studies, the measurement of the T_1, T_2 and M_2 parameters provided information on the structural organization of crystal molecules (M. Adam-Berret et al., 2008). There are many studies that have been performed by different characterization techniques *e.g.* X-ray diffraction (XRD), about the effects of cooling rate on the crystallization behavior of fats. In this study, however, effects of cooling rate changes in meta-stable PKS network were examined by TD LF ^{1}H NMR relaxometry parameters namely T_1, T_2 and M_2. Solid fat content (SFC)s of the samples were also determined by TD LF NMR. The main reason of using TD NMR relaxometry for the detection of crystallization behavior of PKS was to show that NMR relaxometry was able to provide valuable information on the molecular changes within the whole sample volume due to crystallization, in a fast and simple manner, without a detailed peak analysis (Le Botlan, Casseron, & Lantier, 1998). TD NMR relaxometry parameters represent the relaxation behavior of the excited protons within the whole volume of the sample after an applied radio frequency (RF) pulse (Hashemi, Bradley, & Lisanti, 2010). Consequently, NMR relaxometry can also provide more information on the molecular dynamics and the conformational freedom of the molecules with respect to XRD which provides precise atomic details. In this way, NMR relaxometry measurements complement XRD experiments by revealing more information on the changes of molecular dynamics taking place in the bulk of the samples, especially in the liquid state. This also contributes to the determination of the overall crystallization behavior of lipid containing samples (Räntzsch et al., 2018). However, the interpretation of NMR parameters still depends on the comparison with the results of a reliable technique such as XRD (Shukat, Bourgaux, & Relkin, 2012). To the best of our knowledge, there is no study that covers NMR relaxometry parameters to determine the effects of different cooling rates on the crystallization behavior of PKS, complementary to XRD analysis. Hence, the main aim of this study was to show that TD LF NMR measurements could detect the crystallization behavior of PKS with an acceptable accuracy, complementary to the other common techniques. For this purpose, XRD and NMR results were compared with each other to establish a relationship between the parameters of these two non-destructive methods.

2. Materials and methods

2.1. Materials

Palm Kernel Stearin (Cargill, Balıkesir, Turkey) having an iodine value of 5.50 g I_2/100 g and slip melting point (SMP) around 32–33 °C was used in the experiments.

2.2. Sample preparation

PKS samples were heated to 80 °C in water bath and kept for at least 30 min to remove the thermal history of the samples. Then, samples were cooled down to 25 °C at different cooling rates (0.5 °C/min, 3.3 °C/min, 4.7 °C/min and 6.9 °C/min) using a climactaric test cabinet at (Nuve Climatic Test Cabinet, VDW CoolSystems BV, Geldermalsen, Netherlands) and two freezers operating at −18 °C and −80 °C. Time taken to cool from 80 to 25 °C was used to calculate the cooling rate. Samples were analyzed immediately after cooling period.

2.3. X-ray scattering analysis

WAXS measurements were held on HECUS System3 SWAXS system with Cu Kα (λ = 1.54 Å) X-ray source. Measurements were practiced in the 0.77 mbar vacuum environment with 40 mA and 50 kV tube operating conditions. The measurement time for each sample was 400 s. The position-sensitive and 1024-channelled WAXS system is comprised of two linear 1D X-ray detectors accompanied to Kratky type collimator. The channels are 54 μm apart from each other. The monochromatic incident X-rays are used to irradiate the samples and intensity I(q) as a function of the magnitude of X-ray scattering (q) were measured.

2.4. NMR relaxometry experiments

The samples for NMR experiments were prepared by loading 0.8 mL of PKS sample into a 10 mm diameter glass tube. The experiments were carried out via 0.5 T NMR spectrometer operating at the Larmor frequency of 20.34 MHz, equipped with a 10-mm diameter radiofrequency coil (Spin Track, Resonance Systems GmbH, Kirchheim u. Teck, Germany). All NMR experiments were performed at room temperature (25 °C) with three replicates.

2.4.1. Solid fat content (SFC)

SFC measurements were conducted by using the solid echo (SE) sequence as previously performed (Matthieu Adam-Berret, Riaublanc, Rondeau-Mouro, & Mariette, 2009). Measurements were performed at 25 °C. Repetition delay was set to 10 s, the time required to acquire the echo was set to 7 μ s and the number of scans was set to 4.

2.4.2. Crystallinity and second moment (M_2)

In a previous study by Grunin et al. (2019), second moment values of the signal obtained by the Magic Sandwich Echo (MSE) Sequence was used with 10 s repetition delay and 4 scans (Grunin et al., 2019). A special module Relax8 (Resonance Systems GmbH, Kirchheim/Teck, Germany) software calculated the values of the spectral line second moment M_2. From the obtained M_2 values, crystallinity values were calculated by using the calibration curve (crystallinity vs M_2) which was provided in the reference study (Grunin et al., 2019). 512 points were used for the free induction decay (FID) measurements. Readers can also refer to the study of Grunin et al. (2019) for the function that is used to determine the degree of crystallinity and the equation that is used to

calculate M_2.

2.4.3. Longitudinal relaxation time (T_1)

A saturation recovery sequence was used with relaxation period of 1 s, 4 scans and delay time changing between 5 and 1500 ms for 16 points. T_1 values were calculated by fitting the relaxation data to a mono-exponential model using a MATLAB software package (Mathworks Inc., U.S.A). Decay curve results were shown in Supplementary File (Fig. S1).

2.4.4. Spin-spin relaxation time (T_2)

Carr-Purcell-Meiboom-Gill (CPMG) sequence was used to obtain T_2 data with an echo time of 500 μ s, number of echoes 512, relaxation period of 1 s and 16 scans. Decay curves were fitted to a mono-exponential model using MATLAB software package to calculate T_2 values of the samples. Decay curve results were shown in Supplementary File (Fig. S2).

2.5. Statistical analysis

Sigma plot software package (Sigma Plot Ver.14, Chicago, IL, USA) was used to analyze the results. To interpret the effect of cooling rate, one-way ANOVA was used ($p \leq 0.05$). Tukey's multiple comparison test was used to evaluate the significant differences among the different levels of the same factors ($\alpha \leq 0.05$). Also, the Pearson correlation ($\alpha \leq 0.05$) was used to find the correlation coefficients among NMR results.

3. Results and discussion

3.1. X-ray scattering analysis

Wide Angle X-ray scattering (WAXS) technique is used for the determination of lateral chain packing of FAs (polymorphic forms) (Shukat et al., 2012; Toma & Pfohl, 2012). Since polymorphism occurs due to a variety of molecular conformations and molecular packing (lamellar stacking and lateral chain packing), these two levels of organizations are well identified by WAXS measurements. Fatty acid groups of TAGs form three molecular polymorphic conformations; disordered aliphatic chain conformation in α, intermediate packing in β′ and the densest packing in β forms (Sato, 2001). The type of the fat crystal polymorphic form affects the overall quality and acceptability parameters of a food product thus, understanding and controlling the polymorphic behavior of fat crystals within a food product has always been a point of interest (Dian et al., 2017). In many food products such as shortening, butter and margarine, β′ is the desired fat polymorphic form since presence of a high amount of β′ promotes smooth texture. β′ crystals with smaller crystal size than β form, impart more desired crystal network characteristics to the food products. In contrast, β crystals tend to have larger crystal size distribution inducing a rough and grainy texture in foods which could be desirable in a limited number of products such as chocolate (Anihouvi, Blecker, Dombree, & Danthine, 2013). Fig. 1 shows the WAXS patterns of PKS at different cooling rates. According to the study of Shukat et al. (2012), the first peak (at the lowest 'q') belongs to the most stable β polymorphic form. Besides, both the second and fourth peaks represent the β′ polymorphic form and lastly the third peak is related to the least stable α form (Shukat et al., 2012). In order to understand the changes in the content of the polymorphic forms at different cooling rates, percentage areas under each scattering peaks were calculated and the results were demonstrated in Table 1. According to the results, amounts of α and β′ forms increased significantly whereas, a significant decrease in the amount of β form was observed as the cooling rate increased ($p \leq 0.05$). These changes in the crystal morphology were mostly regulated by the different crystal nucleation and growth rates at slow and fast cooling rates (Vuillequez, Koza, Youssef, Bridier, & Saiter, 2010). Rapid cooling enabled the formation of more crystal nucleation sites whereas cooling at slower rates

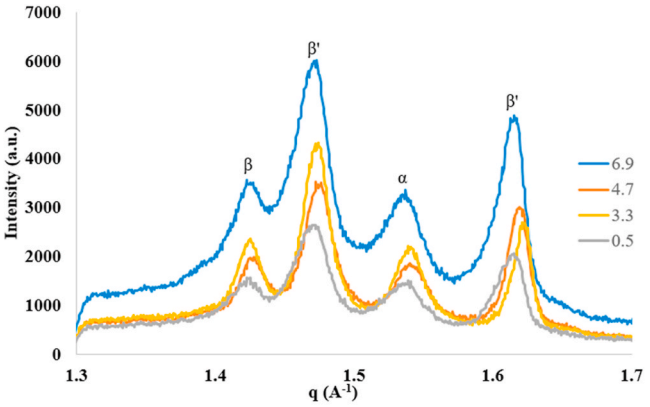

Fig. 1. WAXS profiles of PKS at different cooling rates.

Table 1
Proportions of α, β and β′ polymorphic forms of PKS fat crystals at different cooling rates.

Cooling rate (°C/min)	α (%)	β' (%)	β (%)
0.5	14.68 ± 0.36^{a}	71.08 ± 0.36^{a}	13.77 ± 0.32^{a}
3.3	$15.40 \pm 0.15^{a,b}$	72.63 ± 0.49^{b}	10.91 ± 0.36^{b}
4.7	17.07 ± 0.19^{c}	72.48 ± 0.51^{b}	10.44 ± 0.33^{b}
6.9	17.14 ± 0.18^{c}	75.35 ± 0.38^{c}	9.25 ± 0.36^{c}

Note: Values represented with different superscript letters at each column are statistically different at $p \leq 0.05$.

supported both crystal nucleation and growth with a more predominant crystal growth behavior. As the cooling rate increased, the driving force for the crystal formation also increased substantially (Foubert, Fredrick, Vereecken, Sichien, & Dewettinck, 2008). In contrast, slow cooling provided some time for the TAGs to interact with each other and organize in a more stable conformation (Lopez, Lavigne, Lesieur, Keller, & Ollivon, 2001). This was the main reason for the higher β content at the slowest cooling rate (Table 1). The cooling rate also affects the crystal size distribution of the fat systems. At slow cooling rates, due to the simultaneous crystal nucleation and growth dynamics, a wide size distribution could be observed (Herrera & Hartel, 2000). Additionally, crystals tend to be bigger in size and have needle-shape elements which are the precursors of the β type crystals (Nguyen, Rimaux, Truong, Dewettinck, & Van Bockstaele, 2021). Another important parameter affecting the crystal morphology is the TAG composition of the tested sample. Gregersen et al. (2015) have previously stated that the presence of a mixed TAG composition in a saturated fat resulted in a high degree of variation in the crystal polymorphic forms which was also the case in our study. They have also claimed that stearic acid-rich fats revealed less stable crystal forms *e.g.* α-form, after a rapid cooling process (Gregersen et al., 2015). Higher α crystal content that was observed at the fastest cooling rate (6.9 °C/min) in our study agreed with these findings (Table 1). Despite crystallization into a less stable polymorphic form at higher cooling rates, β′ crystals were the dominant form (71–75%) in PKS at all cooling rates (Table 1). This was related to the β′ crystal forming tendency of lauric fats originating from the presence of TAGs with mixed chain lengths in their structure. Such variations in the FA chain lengths caused some packing problems and formation of crystals having the most stable conformation (β) was prevented (Anihouvi et al., 2013). Therefore, PKS which is a lauric fat, possessed lower amounts of β conformation (9–14%) at all cooling rates studied as shown in Table 1. Although TAGs with similar chain lengths can associate with each other more efficiently and form β crystal conformation during a slow cooling process, variations in the chain lengths of the PKS TAGs reduced the efficiency of this process (Fredrick et al., 2011; X. Zhang et al., 2013). Similar to our results, Vuillequez et al. (2010) have demonstrated that

cooling rate of 3 °C/min was a threshold value in terms of polymorphic behaviors of the stearin fraction of palm oil. Cooling rates above 3 °C/min induced a less stable crystal polymorphic conformation with high α crystal content (Vuillequez et al., 2010). This finding was also consistent with the higher α contents of PKS at the cooling rates above 3 °C/min observed in our study.

3.2. Solid fat content (SFC)

The quantity of fat crystals affects the macroscopic properties of fat crystal networks, and it is determined by SFC (Adam-Berret et al., 2009). SFC is the measure of solid to liquid ratio of a fat containing sample and it has effects on the texture of the final food product (Braipson-Danthine & Deroanne, 2004; Liu et al., 2019). Furthermore, SFC also has an effect on the crystallization characteristics of fats in terms of crystal polymorphisms (Z. Zhang, Shim, Ma, Huang, & Wang, 2018). The SFC results at 25 °C of different cooling rates were shown in Table 2. SFC of PKS increased significantly as the cooling rate increased ($p \leq 0.05$). Apparently, the cooling rate affected the crystal formation rate and behavior as a dynamic factor besides the chemical composition of PKS. Here, the thermodynamic driving force, a high degree of supercooling, induced the increase in SFC (Chaleepa et al., 2010; Herrera & Hartel, 2000). Rapid cooling enhanced the supersaturation of the system and promoted crystal nucleation rate rather than crystal growth rate. Therefore, the formation of a large number of small-size crystals were promoted (Gregersen et al., 2015). Under such cooling conditions, the system was forced to re-organize in crystal form much far from equilibrium which prompted crystal formation in aggregated forms resulting in higher SFC (H. Zhang et al., 2015). These aggregated crystal structures were induced by the rapid undercooling and crystallization of high melting TAGs within the system. The formation of such fat crystals in liquid phase in the early stages of cooling provided nucleation sites for the formation of new crystals which would later rapidly constitute the crystalline lattice (X. Zhang et al., 2013). Additionally, the formation of strong inter-particle links between the crystal clusters at fast cooling conditions may have also contributed to the increasing trend of the SFC values with higher cooling rates (Gregersen et al., 2015). At slow cooling rates, on the other hand, further crystal growth takes place leading to lower SFC due to the production of reduced number of fat crystals (Herrera & Hartel, 2000; Martini, Herrera, & Hartel, 2001).

Besides the effects of cooling rate, all samples had SFC changing between 57 and 61% which could be considered as a high degree range for solid to volume ratio. Previously, stearin-rich fats have also been reported to have SFC around 60% at various cooling rates (Gregersen et al., 2015). A high SFC means a high amount of crystallized fat material in a sample. One main reason for the high SFC of the PKS samples is the presence of a considerable amount of saturated FAs in the TAG composition of PKS (Goon et al., 2019). The low iodine value of the PKS used (~ 5.50 g I_2/100 g) is also consistent with this finding since low iodine values are associated with higher amounts of saturated FA presence in fats (Podchong, Tan, Sonwai, & Rousseau, 2018). Thus, PKS having a high degree of tri-saturated TAGs, were found to have high SFC values (H. Zhang et al., 2015).

Table 2
Solid Fat Content (SFC), Second Moment (M_2) and Degree of Crystallinity results of PKS samples.

Cooling rate (°C/min)	SFC (%)	Second Moment (M_2)	Crystallinity (%)
0.5	57.1 ± 0.2^{d}	12.9 ± 0.01^{d}	61.55 ± 0.13^{d}
3.3	57.6 ± 0.1^{c}	12.94 ± 0.02^{c}	62.14 ± 0.11^{c}
4.7	60.0 ± 0.1^{b}	13.02 ± 0.02^{b}	63.65 ± 0.14^{b}
6.9	60.4 ± 0.2^{a}	14.1 ± 0.06^{a}	72.1 ± 0.01^{a}

Note: Values represented with different superscript letters at each column are statistically different at $p \leq 0.05$.

3.3. Second moment (M_2) and crystallinity analysis

M_2 values were calculated by TD LF ^{1}H NMR measurements in order to understand the dynamics of crystallization and state the degree of crystallinity in PKS samples. M_2 depends both on crystal polymorphism and density but it is nearly not sensitive to crystal size (Matthieu Adam-Berret et al., 2009). Proton mobility and location geometry within a crystal lattice determines the M_2 value of the system (Van Duynhoven, Dubourg, Goudappel, & Roijers, 2002). Therefore, cooling rate has a major effect on the determination of M_2 of a fat containing food formulation. Calculated M_2 values also reveals the degree of crystallinity of the examined system. As shown in Table 2, increasing the cooling rate resulted in higher M_2 and accordingly higher degree of crystallinity for the PKS samples. Higher M_2 at faster cooling rates suggested a more immobile crystal lattice since M_2 is inversely proportional to the proton mobility in solid state (Van Duynhoven et al., 2002). Two factors namely the dominant type of crystal polymorph and overall packing pattern of the crystal organization may have led to this result. Generally, α polymorph is associated with low M_2 since this form exhibits a less compact crystalline organization increasing the mobility of TAGs (M. Adam--Berret et al., 2008). At such mobile crystalline organizations, dipolar interactions between the protons are diminished giving lower M_2 values (Y. L. Wang, Tang, & Belton, 2002). Consequently, these more mobile crystal organizations display a lower degree of crystallinity. On the other hand, β crystals are associated with stronger dipolar interactions thus higher M_2 values (M. Adam-Berret et al., 2008). However, the M_2 results presented in Table 2 were somewhat not in agreement with the aforementioned explanations. As the cooling rate increased, the proportion of the α polymorph increased but M_2 also increased ($p \leq 0.05$). The main reason behind this phenomenon was the increase in crystal nucleation rate at rapid cooling rates which also increased the SFC and overall crystal packing density of the system. The polymorphic form approach was not sufficient to describe the change in M_2 at various cooling rates since the crystallization dynamics of the samples compared were different. A higher amount of solid fat and orderly packed crystal network at rapid cooling rates predominated the proton mobility characteristics of the PKS system. Gregersen et al. (2015) has come to the conclusion that inter-particle interactions between the crystal clusters rather than the intra-particle interactions between the individual crystals determined the crystalline state organization in stearin-rich fats at fast cooling conditions (Gregersen et al., 2015). Rapid cooling provided a more uniform liquid oil distribution between the crystals and the strength of the intra-particle links between the individual crystal particles decreased (Herrera & Hartel, 2000). As a result, the effect of crystal polymorphism on proton mobility diminished at rapid cooling conditions. The high degree of supersaturation induced by rapid cooling was reported to produce branched crystalline pattern that significantly reduced molecular orientational mobility in palm stearin fats, previously (Podchong et al., 2018). In another study, increasing the degree of supercooling decreased the mobility of trilaurin and increased both M_2 and degree of crystallinity as expected (Matthieu Adam-Berret et al., 2009). The same trend was also observed in our study (Table 2). Correlations between SFC, M_2 and crystallinity degree (%) of PKS samples were also checked with Pearson correlation coefficient (r) analysis. There was almost a perfect positive correlation between M_2 and the degree of crystallinity ($r = 0.999$). There were also positive correlations between M_2 and SFC ($r = 0.767$) as well as SFC and degree of crystallinity ($r = 0.771$). In brief, cooling at higher rates increased both SFC, M_2 and degree of crystallinity of PKS. The high degree of crystallinity observed for PKS even at the end of the slowest cooling rate condition (Table 2) could be attributed to the presence of large amount of β′ crystals (~ 71–75%) in the samples as shown in Table 1. This hypothesis was also confirmed by positive correlations between β′ and M_2 ($r = 0.941$) as well as β′ and the degree of crystallinity ($r = 0.950$).

3.4. Analysis of spin-lattice relaxation time

Spin-lattice relaxation time is another parameter that could be utilized to investigate the fat crystal size, polymorphism and properties of the whole crystalline state (M. Adam-Berret et al., 2008; Lucas, Le Ray, Barey, & Mariette, 2005). However, it has been claimed by previous studies that T_1 is more susceptible to changes in crystal size and degree of crystallinity rather than to morphology of the crystals (Matthieu Adam-Berret et al., 2009; H. Zhang et al., 2015). There are also some studies claiming that T_1 could be used to make a distinction between the fat crystal polymorphs depending on the changes of the mobility and compactness of the polymorphs analyzed (M. Adam-Berret et al., 2008; Eads, Blaurock, Bryant, Roy, & Croasmun, 1992). The ambiguity on the issue arises from the differences in the solid to liquid ratio and the solid-state conformations of the samples used in different studies. Generally, T_1 of an overall system which is composed of solid and liquid portions, depends on molecular mobility but compactness and conformation of the solid state has also a major influence on T_1 especially at high SFCs (>50%). For instance, a more compact and highly ordered solid state may generate an increase in T_1 (Matthieu Adam-Berret et al., 2009). Crystal size and thickness was also reported to change T_1 but this is applicable for the systems with low SFC (<50%). For such low SFC systems, an increase in crystal size was associated with an increase in T_1 (Lubach, Xu, Segmuller, & Munson, 2007). There was also an increase in T_1 of the PKS samples as the cooling rate increased as shown in Fig. 2. However, this increasing trend of T_1 was mostly related to the simultaneous increase in SFC and crystallinity (%) values (Table 2). At the highest cooling rate level (6.9 °C/min), SFC demonstrated an increase of 3% whereas a more striking rise in crystallinity (~ 11%) was observed. The steeper increase in crystallinity was the result of tight and dense crystal lattice arrangement at high cooling rates especially at 6.9 °C/min. The compact solid network which was induced by high crystal nucleation rate reduced the molecular mobility within the system. Therefore, immobile fat crystals were not able to transfer their energy to the surrounding lattice, efficiently (Matthieu Adam-Berret, Boulard, Riaublanc, & Mariette, 2011). Consequently, spin-lattice relaxation rate of the system decreased and a longer T_1 was observed. Another factor contributed to the reduction of the spin-lattice relaxation rate of the system was the changes in the spin diffusion process. Crystal organizations with higher mobility may have some specific fast relaxing regions which can also contribute to the overall relaxation of the system by transferring the magnetization of slow relaxing regions via spin diffusion process. Such fast relaxing regions could be in the form of crystal defect sites and crystal surfaces (Matthieu Adam-Berret et al., 2009). In this way, spin diffusion reduces T_1. Nevertheless, PKS samples experienced a more compact, immobile and smooth crystalline state with less imperfections as the cooling rate increased, revealing an increasing trend for T_1 (Fig. 2). Strong positive Pearson correlations (r) found such as r's of 0.919, 0.926 and 0.932 between T_1-SFC, T_1-M_2 and T_1-crystallinity (%), respectively, also supported our claims.

3.5. Spin-spin relaxation time of the liquid fraction

Spin-spin relaxation time detects the variances in the degree of mobility of spins within a system and it is a property for both solid and liquid phases. For solid we use M_2 instead of T_2, because it gives better fitting. For liquid measurements we utilize CPMG (CPMG cannot look inside the crystal, because echo time is much higher than the relaxation of crystal). Despite low T_2 values in solid state, transverse relaxation process is sensitive to the changes in the rigid crystalline conformations and polymorphic form of the fat crystals (Van Duynhoven et al., 2002). Additionally, the most dominant factor affecting T_2 is SFC (Matthieu Adam-Berret et al., 2011). Contrary to the relationship between SFC and T_1, T_2 and SFC are inversely proportional to each other. If the fat crystal clusters constituting the whole fat network are in straight and parallel conformation as suggested by Tang and Marangoni (2008), the overall system could be considered as an interconnected porous medium (Tang & Marangoni, 2008). In this model, fat crystals are interconnected with each other and in the pores between the connected crystals, liquid oil resides (Liang, Shi, & Hartel, 2008). Here, the surface relaxation mechanism predominates the spin-spin relaxation behavior of the entire system. At high cooling rates, a great number of small crystals were formed increasing the surface to volume ratio of the crystalline state which was also validated by the increase in SFC (Table 2). Therefore, the total crystal surface area interacting with the liquid oil phase residing in the pores of the crystalline network increased (Matthieu Adam-Berret et al., 2011). Evolution of crystals in the bulk liquid oil phase at the high cooling rates due to immense crystal nucleation rate could also contribute to the higher spin-spin relaxation rates at such cooling conditions (Matthieu Adam-Berret et al., 2011). All these phenomena that took place at high cooling rates may have also led to an increase in the overall viscosity of the PKS sample (X. Zhang et al., 2013). The high viscosity may be also one of the reasons for low T_2 and reduced the mobility of the TAG chains restricting the rearrangement capability of the formed crystals. Without the further rearrangements in the crystalline state, TAGs formed a more proportion of unstable (α) crystals (Kellens, Meeussen, & Reynaers, 1990; X.; Zhang et al., 2013).

The longer T_2 observed at the slowest cooling rate (0.5 °C/min) as shown in Fig. 3 was also related to the fat crystal morphology. The slow cooling process provided some time for crystals to grow. Consequently, surface to volume ratio of the crystal system decreased which increased the T_2 (Matthieu Adam-Berret et al., 2011). Growth of the crystals also increased the proportion of β conformation of the crystals (Table 1) due

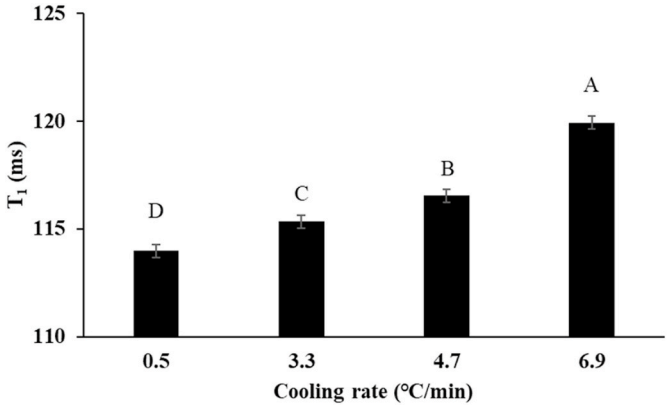

Fig. 2. Longitudinal relaxation time (T_1) results of PKS samples at different cooling rates. Errors are represented as standard errors with significant differences ($p \leq 0.05$) indicated by capital letters.

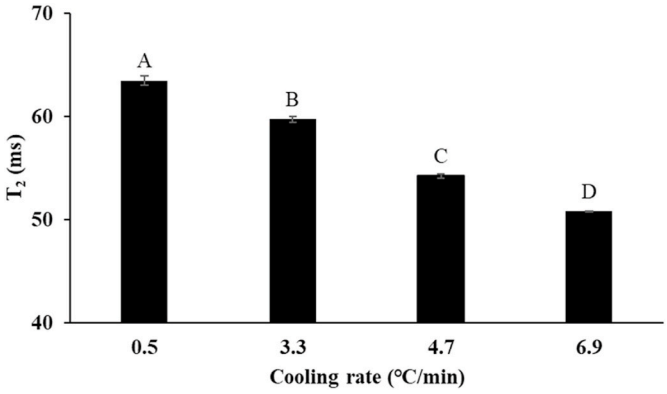

Fig. 3. Transverse relaxation time (T_2) results of PKS samples at different cooling rates. Errors are represented as standard errors with significant differences ($p \leq 0.05$) indicated by capital letters.

to the more time available for molecular arrangements (Sato, 2001). The close and compact crystal alignment provided by β conformation promoted the expelling of liquid oil from the highly ordered crystal lattice. Thus, the ratio of the liquid oil surrounding the crystals increased, giving longer T_2 since a higher spin-spin relaxation time is observed at higher liquid proportions (Mazzanti, Mudge, & Anom, 2008). Strong positive Pearson correlations (r) found between β obtained from WAXS measurements and T_2 ($r = 0.927$). Spin-spin relaxation results showed that a change in the crystal conformation from the α to β affected the liquid distribution in the sample volume and the resulting relaxation behavior.

4. Comments

In food industry, control of fat crystallization is an important factor to be sure about the physicochemical properties of fat-based products. Cooling rate is one of the important parameters affecting fat crystallization behaviors. NMR is a non-destructive method that can be used to detect the physicochemical changes in foods. As far as we know, there is no study in literature related to effects of different cooling rates on crystallization behavior of PKS explained by NMR relaxometry parameters. The results showed that SFC, T_1, degree of crystallinity and M_2 increased as the cooling rate increased. In contrast, shorter T_2 values were observed at higher cooling rates. Moreover, X-ray scattering experiments indicated that cooling rate also modified the polymorphism of TAGs. The least stable α polymorph formed upon fast cooling. It was alo possible to connect X-ray scattering findings and ^{1}H NMR relaxometry results. For instance, a higher β crystal content also revealed a longer T_2. The reason could be the expulsion of liquid oil from the highly ordered crystalline state formed in the presence of β crystals. In this way, the contribution of the liquid oil fraction to spin – spin relaxation probably became greater due to the increase in their molecular freedom. To conclude, NMR relaxometry can be used as a tool to interpret the crystallization behavior of PKS complementary to X-ray scattering.

CRediT authorship contribution statement

Ilhami Okur, Purlen Sezer and Derya Ucbas conducted the experiments.

Ilhami Okur and Baris Ozel drafted the manuscript and Baris Ozel revised it.

Dr. Alpas has gone through the 1st draft.

Dr. Side helped in the WAXS experiments.

Dr. Grunin has designed the software and analysis tool for crystallinity measurements.

Dr. Oztop finalized the study.

Declaration of competing interest

All the authors have approved the manuscript and agree with the submission. There are no conflicts of interest to declare.

Acknowledgments

This study was funded from Dr. Oztop's award of Science Academy's Young Scientist Awards Program (BAGEP).

Appendix A. Supplementary data

Supplementary data to this article can be found online at https://doi.org/10.1016/j.lwt.2021.113001.

References

Adam-Berret, M., Boulard, M., Riaublanc, A., & Mariette, F. (2011). Evolution of fat crystal network microstructure followed by NMR. *Journal of Agricultural and Food Chemistry, 59*(5), 1767–1773. https://doi.org/10.1021/jf102734d

Adam-Berret, M., Riaublanc, A., Rondeau-Mouro, C., & Mariette, F. (2009). Effects of crystal growth and polymorphism of triacylglycerols on nmr relaxation parameters. 1. evidence of a relationship between crystal size and spin-lattice relaxation time. *Crystal Growth & Design, 9*(10), 4273–4280. https://doi.org/10.1021/cg900218f

Adam-Berret, M., Rondeau-Mouro, C., Riaublanc, A., & Mariette, F. (2008). Study of triacylglycerol polymorphs by nuclear magnetic resonance: Effects of temperature and chain length on relaxation parameters. *Magnetic Resonance in Chemistry, 46*(6), 550–557. https://doi.org/10.1002/mrc.2213

Alacik Develioglu, I., Ozel, B., Sahin, S., & Oztop, M. H. (2020). NMR Relaxometry and magnetic resonance imaging as tools to determine the emulsifying characteristics of quince seed powder in emulsions and hydrogels. *International Journal of Biological Macromolecules, 164*, 2051–2061. https://doi.org/10.1016/j.ijbiomac.2020.08.087

Anihouvi, P. P., Blecker, C., Dombree, A., & Danthine, S. (2013). Comparative study of thermal and structural behavior of four industrial lauric fats. *Food and Bioprocess Technology, 6*(12), 3381–3391. https://doi.org/10.1007/s11947-012-0980-9

Braipson-Danthine, S., & Deroanne, C. (2004). Influence of SFC, microstructure and polymorphism on texture (hardness) of binary blends of fats involved in the preparation of industrial shortenings. *Food Research International, 37*(10), 941–948. https://doi.org/10.1016/j.foodres.2004.06.003

Chaleepa, K., Szepes, A., & Ulrich, J. (2010). Effect of additives on isothermal crystallization kinetics and physical characteristics of coconut oil. *Chemistry and Physics of Lipids, 163*(4–5), 390–396. https://doi.org/10.1016/j.chemphyslip.2010.03.005

Dian, N. L. H. M., Hamid, R. A., Kanagaratnam, S., Isa, W. R. A., Hassim, N. A. M., Ismail, N. H., et al. (2017). Palm oil and palm kernel oil: Versatile ingredients for food applications. *Journal of Oil Palm Research, 29*(4), 487–511. https://doi.org/10.21894/jopr.2017.00014

Eads, T. M., Blaurock, A. E., Bryant, R. G., Roy, D. J., & Croasmun, W. R. (1992). Molecular motion and transitions in solid tripalmitin measured by deuterium nuclear magnetic resonance. *Journal of the American Oil Chemists' Society, 69*(11), 1057–1068. https://doi.org/10.1007/BF02541038

Foubert, I., Fredrick, E., Vereecken, J., Sichien, M., & Dewettinck, K. (2008). Stop-and-return DSC method to study fat crystallization. *Thermochimica Acta, 471*(1–2), 7–13. https://doi.org/10.1016/j.tca.2008.02.005

Fredrick, E., Van De Walle, D., Walstra, P., Zijtveld, J. H., Fischer, S., Van der Meeren, P., et al. (2011). Isothermal crystallization behaviour of milk fat in bulk and emulsified state. *International Dairy Journal, 21*(9), 685–695. https://doi.org/10.1016/j.idairyj.2010.11.007

Goon, D. E., Abdul Kadir, S. H. S., Latip, N. A., Rahim, S. A., & Mazlan, M. (2019). Palm oil in lipid-based formulations and drug delivery systems. *Biomolecules, 9*(2), 1–19. https://doi.org/10.3390/biom9020064

Gregersen, S. B., Miller, R. L., Hammershøj, M., Andersen, M. D., & Wiking, L. (2015). Texture and microstructure of cocoa butter replacers: Influence of composition and cooling rate. *Food Structure, 4*, 2–15. https://doi.org/10.1016/j.foostr.2015.03.001

Grunin, L., Oztop, M. H., Guner, S., & Baltaci, S. F. (2019). Exploring the crystallinity of different powder sugars through solid echo and magic sandwich echo sequences. *Magnetic Resonance in Chemistry, 57*(9), 607–615. https://doi.org/10.1002/mrc.4866

Hashemi, R. H., Bradley, W. G., & Lisanti, C. J. (2010). *Mri: The basics* (3rd ed.). Baltimore: Lippincott Williams and Wilkins.

Herrera, M. L., & Hartel, R. W. (2000). Effect of processing conditions on physical properties of a milk fat model system: Microstructure. *Journal of the American Oil Chemists' Society, 77*(11), 1197–1205. https://doi.org/10.1007/s11746-000-0186-2

Himawan, C., Starov, V. M., & Stapley, A. G. F. (2006). Thermodynamic and kinetic aspects of fat crystallization. *Advances in Colloid and Interface Science, 122*(1–3), 3–33. https://doi.org/10.1016/j.cis.2006.06.016

Kellens, M., Meeussen, W., & Reynaers, H. (1990). Crystallization and phase transition studies of tripalmitin. *Chemistry and Physics of Lipids, 55*(2), 163–178. https://doi.org/10.1016/0009-3084(90)90077-5

Kirtil, E., & Oztop, M. H. (2016). 1H nuclear magnetic resonance relaxometry and magnetic resonance imaging and applications in food science and processing. *Food Engineering Reviews*. https://doi.org/10.1007/s12393-015-9118-y

Le Botlan, D., Casseron, F., & Lantier, F. (1998). Polymorphism of sugars studied by time domain NMR. *Analysis, 26*(5), 198–204. https://doi.org/10.1051/analusis:1998135

Liang, B., Shi, Y., & Hartel, R. W. (2008). Correlation of rheological and microstructural properties in a model lipid system. *Journal of the American Oil Chemists' Society, 85*(5), 397–404. https://doi.org/10.1007/s11746-008-1213-2

Liu, C., Meng, Z., Chai, X., Liang, X., Piatko, M., Campbell, S., et al. (2019). Comparative analysis of graded blends of palm kernel oil, palm kernel stearin and palm stearin. *Food Chemistry, 286*(September 2018), 636–643. https://doi.org/10.1016/j.foodchem.2019.02.067

Lopez, C., Lavigne, F., Lesieur, P., Keller, G., & Ollivon, M. (2001). Thermal and structural behavior of anhydrous milk fat. 2. Crystalline forms obtained by slow cooling. *Journal of Dairy Science, 84*(11), 2402–2412. https://doi.org/10.3168/jds.S0022-0302(01)74689-9

Lubach, J. W., Xu, D., Segmuller, B. E., & Munson, E. J. (2007). Investigation of the effects of pharmaceutical processing upon solid-state NMR relaxation times and implications to solid-state formulation stability. *Journal of Pharmaceutical Sciences, 96*(4), 777–787. https://doi.org/10.1002/jps.20684

Lucas, T., Le Ray, D., Barey, P., & Mariette, F. (2005). NMR assessment of ice cream: Effect of formulation on liquid and solid fat. *International Dairy Journal, 15*(12), 1225–1233. https://doi.org/10.1016/j.idairyj.2004.06.012

Maleky, F., Acevedo, N. C., & Marangoni, A. G. (2012). Cooling rate and dilution affect the nanostructure and microstructure differently in model fats. *European Journal of Lipid Science and Technology, 114*(7), 748–759. https://doi.org/10.1002/ejlt.201100314

Martini, S., Herrera, M. L., & Hartel, R. W. (2001). Effect of cooling rate on nucleation behavior of milk fat - sunflower oil blends. *Journal of Agricultural and Food Chemistry, 49*(7), 3223–3229. https://doi.org/10.1021/jf001101j

Mazzanti, G., Mudge, E. M., & Anom, E. Y. (2008). In situ rheo-NMR measurements of solid fat content. *Journal of the American Oil Chemists' Society, 85*(5), 405–412. https://doi.org/10.1007/s11746-008-1227-9

Nguyen, V., Rimaux, T., Truong, V., Dewettinck, K., & Van Bockstaele, F. (2021). The effect of cooling on crystallization and physico-chemical properties of puff pastry shortening made of palm oil and anhydrous milk fat blends. *Journal of Food Engineering, 291*, 110245. https://doi.org/10.1016/j.jfoodeng.2020.110245. July 2020.

Norizzah, A. R., Nur Azimah, K., & Zaliha, O. (2018). Influence of enzymatic and chemical interesterification on crystallisation properties of refined, bleached and deodourised (RBD) palm oil and RBD palm kernel oil blends. *Food Research International, 106*(January), 982–991. https://doi.org/10.1016/j.foodres.2018.02.001

Podchong, P., Tan, C. P., Sonwai, S., & Rousseau, D. (2018). Composition and crystallization behavior of solvent-fractionated palm stearin. *International Journal of Food Properties, 21*(1), 496–509. https://doi.org/10.1080/10942912.2018.1425701

Räntzsch, V., Haas, M., Özen, M. B., Ratzsch, K. F., Riazi, K., Kauffmann-Weiss, S., et al. (2018). Polymer crystallinity and crystallization kinetics via benchtop 1H NMR relaxometry: Revisited method, data analysis, and experiments on common polymers. *Polymer, 145*, 162–173. https://doi.org/10.1016/j.polymer.2018.04.066

Sato, K. (2001). Crystallization behaviour of fats and lipids - a review. *Chemical Engineering Science, 56*(7), 2255–2265. https://doi.org/10.1016/S0009-2509(00)00458-9

Sato, K., Bayés-García, L., Calvet, T., Cuevas-Diarte, M.À., & Ueno, S. (2013). External factors affecting polymorphic crystallization of lipids. *European Journal of Lipid Science and Technology, 115*(11), 1224–1238. https://doi.org/10.1002/ejlt.201300049

Shukat, R., Bourgaux, C., & Relkin, P. (2012). Crystallisation behaviour of palm oil nanoemulsions carrying vitamin E: DSC and synchrotron X-ray scattering studies. *Journal of Thermal Analysis and Calorimetry, 108*(1), 153–161. https://doi.org/10.1007/s10973-011-1846-5

Tang, D., & Marangoni, A. G. (2008). Modified fractal model and rheological properties of colloidal networks. *Journal of Colloid and Interface Science, 318*(2), 202–209. https://doi.org/10.1016/j.jcis.2007.09.062

Toma, A. C., & Pfohl, T. (2012). Small-angle X-ray scattering (SAXS) and wide-angle X-ray scattering (WAXS) of supramolecular assemblies. *Supramolecular Chemistry*. https://doi.org/10.1002/9780470661345.smc042

Van Duynhoven, J., Dubourg, I., Goudappel, G. J., & Roijers, E. (2002). Determination of MG and TG phase composition by time-domain NMR. *JAOCS, Journal of the American Oil Chemists' Society, 79*(4), 383–388. https://doi.org/10.1007/s11746-002-0493-7

Vuillequez, A., Koza, L., Youssef, B., Bridier, M., & Saiter, J. M. (2010). Thermal and structural behavior of palm oil. Influence of cooling rate on fat crystallization. *Macromolecular Symposia, 290*(1), 137–145. https://doi.org/10.1002/masy.201050416

Wang, F., Liu, Y., Jin, Q., Huang, J., Meng, Z., & Wang, X. (2011). Kinetic analysis of isothermal crystallization in hydrogenated palm kernel stearin with emulsifier mixtures. *Food Research International, 44*(9), 3021–3025. https://doi.org/10.1016/j.foodres.2011.07.014

Wang, Y. L., Tang, H. R., & Belton, P. S. (2002). Solid state NMR studies of the molecular motions in the polycrystalline α-L-fucopyranose and methyl α-L-fucopyranoside. *Journal of Physical Chemistry B, 106*(49), 12834–12840. https://doi.org/10.1021/jp0268617

Zhang, X., Li, L., Xie, H., Liang, Z., Su, J., Liu, G., et al. (2013). Comparative analysis of thermal behavior, isothermal crystallization kinetics and polymorphism of palm oil fractions. *Molecules, 18*(1), 1036–1052. https://doi.org/10.3390/molecules18011036

Zhang, Z., Shim, Y. Y., Ma, X., Huang, H., & Wang, Y. (2018). Solid fat content and bakery characteristics of interesterified beef tallow-palm mid fraction based margarines. *RSC Advances, 8*(22), 12390–12399. https://doi.org/10.1039/c8ra00769a

Zhang, H., Zhang, L., Sun, X., & Xie, S. (2015). Applications of low-field pulsed nuclear magnetic resonance technique in lipid and food. In A.-ur Rahman, & M. I. Choudhary (Eds.), *Applications of NMR spectroscopy* (1st ed.,, *1* pp. 3–56). Elsevier Ltd. https://doi.org/10.1016/B978-1-60805-963-8.50001-9.